
**Separation Science and Technology**
Publication details, including instructions for authors and subscription information:
http://www.informaworld.com/smpp/title~content=t713708471

# Preparation and Characterizations of Ceramic Microfiltration Membrane: Effect of Inorganic Precursors on Membrane Morphology

Somen Jana[a]; M. K. Purkait[a]; Kaustubha Mohanty[a]
[a] Department of Chemical Engineering, Indian Institute of Technology Guwahati, Guwahati, India

Online publication date: 20 December 2010

**To cite this Article** Jana, Somen , Purkait, M. K. and Mohanty, Kaustubha(2011) 'Preparation and Characterizations of Ceramic Microfiltration Membrane: Effect of Inorganic Precursors on Membrane Morphology', Separation Science and Technology, 46: 1, 33 — 45
**To link to this Article: DOI:** 10.1080/01496395.2010.503669
**URL:** http://dx.doi.org/10.1080/01496395.2010.503669

*Separation Science and Technology*, 46: 33–45, 2011

ISSN: 0149-6395 print/1520-5754 online
DOI: 10.1080/01496395.2010.503669

Taylor & Francis
Taylor & Francis Group

# Preparation and Characterizations of Ceramic Microfiltration Membrane: Effect of Inorganic Precursors on Membrane Morphology

**Somen Jana, M. K. Purkait, and Kaustubha Mohanty**
*Department of Chemical Engineering, Indian Institute of Technology Guwahati, Guwahati, India*

**Ceramic disc type microfiltration membranes (50 mm diameter and 5 mm thickness) were prepared by the paste method from different compositions of clay, kaolin, and binding agents like sodium carbonate, sodium metasilicate, boric acid, and sintered at different temperatures. All the membranes were characterized by TGA, SEM, XRD, water permeability test, and acid–base treatment. With the increase of sintering temperature, the pore size as well as the permeability and flexural strength were increasing while porosity and pore density were decreasing. It was found that with increasing the amount of kaolin and decreasing the amount of clay the pore diameter was decreasing. A membrane prepared from 18% clay, 62% kaolin, and 20% binding material and sintered at 1000°C has shown the lowest average pore size of 0.31 μm with porosity, pore density, and flexural strength of 0.22, $4.80 \times 10^{12}\,m^{-2}$ and 12.81 MPa respectively. The membrane pore size and pore density were predicted directly from the particle size distribution of the clay and kaolin and were suitably represented by second-order polynomials.**

**Keywords** ceramic membrane; clay; microfiltration; pore size prediction



## INTRODUCTION

In the past two decades membrane technology has significantly progressed. Many applications were proposed where microfiltration and ultrafiltration were applied, like biotechnology (1), wastewater treatment (2), fruit juice clarification (3), wine filtration (4), fermentation broth clarification (5). These technologies are regarded as economically competitive due to the availability of membranes with higher flux and lower process cost. Recently ceramic membranes are drawing a lot of attraction due to their advantages like resistance to corrosive feed, high temperature and high pressure applications, and long life. On the other hand, ceramic membranes are at least ten times costlier than polymeric membranes. Different types of morphology, stability, and porous texture of inorganic membranes were created with a different combination of precursors with a final aim of good separation characteristics. Precursors were aggregated by the paste method or uniaxial pressing to the desired shape of the membrane followed by sintering (6,7). Different raw materials as precursors have different functional attributes for the membrane structure. Kaolin provides low plasticity and high refractory properties to the membrane. Quartz provides thermal and mechanical stability. Calcium carbonate during sintering evolves $CO_2$ thus creating porous texture in the ceramics. Sodium metasilicate increases mechanical strength by creating silicate bonds. Sodium carbonate improves dispersion properties, thereby creating homogeneity. Boric acid also increases mechanical strength by creating metaborates during sintering (8).

During the early research on ceramic membrane preparation, expensive alumina powder was used as the main precursor. DeFriend et al. (9) reported a pore size of 15–25 nm from the $\alpha$-alumina powder with an average particle size of 15–40 nm. Afterwards, Falamaki et al. (10) obtained a pore size of around 0.5 μm from 160 μm average particle sized $\gamma$-alumina powder. However, the cost of such precursors remains a cause of concern. Search for cheaper raw materials ended with the use of titania powder (pore size 0.1–0.2 μm; precursor size: 0.37 μm), apatite powder (pore size 5–7 μm; grain size: 50–350 μm), natural clay (pore size 9–10 μm; grain size: 9 μm) etc for the preparation of ceramic membrane (11–13). Nandi et al (14). prepared ceramic membrane using kaolin as the main raw material. The pore sizes reported were 0.75–1.5 μm for the average particle size of 5 μm. Das et al. (15) had shown that the particle size and its distribution of membrane preparing materials have an important effect on the pore size, pore size distribution, and porosity of the membrane. Apart from these, the effect of sintering temperature on the pore diameter was also studied (16). In general the pore size increases with the increase of the sintering temperature. This happens partially due to the overlapping of the small sized pores by large sized pores during sintering. Saffaj et al.

Received 12 March 2010; accepted 21 June 2010.
Address correspondence to Kaustubha Mohanty and Dr. M. K. Purkait, Department of Chemical Engineering, Indian Institute of Technology Guwahati, Guwahati – 781039, India. Tel.: +91-361-2582267/62; Fax: +91-361-2582291. E-mail: kmohanty@iitg.ernet.in

(16) reported the increase of the pore size from 9.4 μm to 10.8 μm during the increase of the sintering temperature from 1100°C to 1250°C for membranes prepared from natural clay. According to Masmoudi et al. (12) the pore size was increased from 5 μm to 7 μm during the increase of the temperature from 1150°C to 1200°C for the membranes prepared from apatite powder.

Critical review of the above works reveals that the most important controlling parameter for pore size variation is the particle size of the membrane precursor, though sintering temperature also plays an important role. Most of the literatures focused on the variation of pore diameter with sintering temperatures. Very few literatures discussed the role of membrane precursor diameter on the membrane pore size (15). Moreover, the relationship of the surface weighted mean diameter [$D_{3,2}$], volume weighted mean diameter [$D_{4,3}$] of the particle size distribution (PSD) with the pore size and the variation of the pore density with PSD were not studied yet.

The objective of the present work is to prepare membranes with wide ranges of pore size using different PSD of the membrane precursor and to find a suitable relation of the pore size with PSD of the membrane precursor. The precursors with different average particle size were prepared by mixing kaolin and clay powder in different ratios. Characterization of the prepared membranes by TGA, SEM, XRD, the water permeability test, and acid–base treatment for analyzation of different membrane morphological parameters were also studied. A relationship was developed to predict the membrane pore size from the PSD of the membrane precursor.



## MATERIALS AND METHODS

### Raw Materials

– 150 mesh natural clay (collected from IIT Guwahati campus) was used as clay powder. The chemical analysis was done by X-ray fluorescence (Philips, PW 2440 MagiX-PRO). Clay powder and kaolin (CDH (P.) Ltd.) were used for the preparation of the membranes where as sodium metasilicate (Loba Chemie Pvt. Ltd.), sodium carbonate (Rankem, India) and boric acid (Loba Chemie Pvt. Ltd.) were used as binding materials.

### Membrane Preparation and Characterization

Membranes were prepared by paste casting as per the compositions given in Table 1. The compositions were not chosen randomly; rather those were determined by the trial-and-error method. Several membranes having a different composition were prepared and characterized. In some cases membranes were not formed at all; sometimes membranes formed are of distorted in shape. After many trials the composition reported here was found to be the best. During the selection of various compositions, we have considered the role of different membrane forming precursors. For example, the binding materials (sodium carbonate, sodium metasilicate, and boric acid) provide mechanical strength to the membranes; use of less amount of binding material makes the membrane brittle. On the other hand, excess use of binding material may lead to many problems like, the binding materials may come out from the membrane during sintering or it can stick to the furnace floor. The materials were mixed with distilled water and the paste was casted over a gypsum surface in the shape of a circular disc of 52 mm diameter and 6 mm thickness by a dice made from perspex sheet. After partial drying at room temperature for 24 h, the disc was removed carefully and heated at 100°C for 12 h. Eventually, the casted disc was heated step by step (50°C in every 15 min) in a programmable muffle furnace (Naskar & Co.; 140QT) to the desired sintering temperature and kept at this temperature for 6 h. Then, the temperature of the muffle furnace was cooled gradually to room temperature. Finally, the membrane was polished with silicon carbide abrasive paper (C-180) to give a final shape of around 50 mm diameter and 5 mm thickness as well as washed in distilled water and dried. Membrane A, B, C, and D were prepared at 1000°C. Membrane E was sintered at different temperature (850°C, 900°C, 950°C and 1000°C) for observing the effect of temperature on the pore size of the membrane.

TABLE 1
Different compositions (dry basis) of raw materials used for preparing membranes

| | Membrane material | | Binding material | | | |
|---|---|---|---|---|---|---|
| Compositions | Clay (%) | Kaolin (%) | Sodium carbonate (%) | Sodium metasislicate (%) | Boric acid (%) | % of binding material used |
| Membrane A | 92 | 0 | 4 | 2 | 2 | 8 |
| Membrane B | 70 | 18 | 6 | 3 | 3 | 12 |
| Membrane C | 50 | 34 | 8 | 4 | 4 | 16 |
| Membrane D | 32 | 50 | 9 | 4.5 | 4.5 | 18 |
| Membrane E | 18 | 62 | 10 | 5 | 5 | 20 |

For the analysis of thermal transformations during the whole sintering process, thermo-gravimetric analysis (TGA) (Mettler-851e) of all the compositions were conducted from 30°C to 950°C. All membranes were investigated by XRD (Bruke D8, advanced X-ray diffraction measurement system) to study the phase changes and SEM (Leo 1430 vp) to determine average pore size and pore size distribution. The porosity and flexural strength (Universal tensile testing machine, Dutt- 101) were also determined. Water permeation experiments were carried out to evaluate the average pore size and permeability. Chemical stability of the membranes was checked by comparing the porosity, pore size, permeability, and mechanical strength before and after acid and base treatment. This was done by immersing the membranes in a solution of NaOH (pH = 13.5) and HCl (pH = 1.0) separately for 72 h.

All membranes were subjected to water permeation experiments using deionized water. Hydraulic permeability ($L_h$) and average pore diameter ($r_l$) were determined by Eq. (1):

$$J = \frac{n\pi r^4 \Delta P}{8\mu l} = L_h \Delta P \tag{1}$$

where, J is the liquid flux ($m^3 m^{-2} s^{-1}$), ΔP is the transmembrane pressure (Pa), $\mu$ is the viscosity of water, and $l$ the pore length (i.e., thickness of membrane, assuming the pores are cylindrical) (6). Taking porosity, $\varepsilon = n\pi r^2$ ($n$ = number of pores per unit area and $r$ = radius of pore), Eq. (1) can be rewritten as:

$$r_l = \left[\frac{8\mu l L_h}{\varepsilon}\right]^{0.5} \tag{2}$$

The porosity was measured by the pycnometric method using water as the wetting liquid (14). The transmembrane pressure drop for water permeability experiments was in the range of 34–482 kPa for different membranes. Before the experiment, standard compaction tests were conducted at a pressure which was above the operating pressure. For membrane B, the operating pressure was 34–138 kPa and the compaction was done at 165 kPa. The flux was initially high and reduced to a steady value in 2–3 h. These data were obtained by measuring the permeate volume in every 10 s. For membrane A, the flux decline was 8.2%, whereas for membrane E, the flux decline was 48.5% with respect to the initial flux. This is due to the squeezing of the pore structure under pressure. Other researchers also reported similar results for ceramic membranes prepared from kaolin, silica, and calcium carbonate (14). In the next stage of the experiment, the flux through the membrane was measured with respect to different pressures. From the slope of ΔP vs. J ($R^2$ values were between 0.97 and 0.99), the hydraulic permeability ($L_h$) was obtained by using Eq. (1). With this value and porosity value, the average pore radius was calculated from Eq. (2).

## Relationship between PSD of Membrane Precursor with Membrane Pore Size and Pore Density

Mixtures of kaolin and clay powder in different compositions were used for obtaining different particle size distribution (PSD) and average particle size of the membrane precursor. PSD of all the mixture of clay and kaolin were determined by Laser Particle Size Analyzer (Malvern, Masterizer-2000). The values of the average particle diameter [$D_{1,0}$], surface weighted mean diameter [$D_{3,2}$], volume weighted mean diameter [$D_{4,3}$], and the specific area for all the mixtures were directly obtained from the PSD report, whereas, the mean diameter quantities were calculated by the following formulae:

$$D_{1,0} = \frac{\sum n_i d_i}{\sum n_i} \tag{3}$$

$$D_{3,2} = \frac{\sum n_i d_i^3}{\sum n_i d_i^2} \tag{4}$$

$$D_{4,3} = \frac{\sum n_i d_i^4}{\sum n_i d_i^3} \tag{5}$$

Here $n_i$ means the (number-based) frequency of occurrence of particles in size class $i$, having a mean diameter $d_i$ (17) The spread of the particle size distribution of the powders was expressed by "quartile ratio" which represents the size ratio corresponding to the cumulative finer percentage of 75 and 25 in the particle size distribution curve (15). The relationship of the average pore size with $D_{1,0}$, $D_{3,2}$, $D_{4,3,}$ and the specific area and the relationship of pore density with respect to the average particle diameter and quartile ratio were determined. For this, first the values were plotted in MS Excel 2003. Afterwards, different correlations were checked by comparing the $R^2$ values for finding the best correlation.

## Confidence Interval

In statistics, confidence intervals (CI) estimate and represent uncertainty or imprecision associated with estimates of population parameters from sample data. Instead of estimating the parameter by a single value, the parameter is represented by an interval. In that way, confidence intervals indicate the reliability of an estimate.

A confidence interval always presents a particular confidence level, usually expressed as a percentage. The end points of the confidence interval are referred to as confidence limits. Increase in the desired confidence level will increase the confidence interval. Ninety-five percent

confidence intervals for all the developed relationships were determined by MS-Excel-2007 with regression analysis.

## RESULTS AND DISCUSSIONS

### Clay and Kaolin Properties

Basic properties of clay like pH (6.6), bulk density (1230 kg m$^{-3}$), organic matter (0.96%), and soluble matter (3.0%) were obtained. Standard methodologies were followed for calculating these properties (18). The total component analysis (X-Ray Fluorescence report) of clay is shown in Table 2. Kaolin was mixed with clay in different ratios for making membranes of different pore size. The PSD of different membrane precursors and kaolin are shown in Fig. 1. It can be seen that kaolin has much finer particles than clay. The average particle size was decreasing as compositions were varied from A to E. For membrane A, B, C, D, and E, the average particle size was 34.66 μm, 30.37 μm, 26.07 μm, 21.79 μm, and 17.51 μm respectively.

### Structural Characterization of Prepared Membrane

*Thermo-Gravimetric Analysis*

As a general observation, mass loss was increased with the successive compositions (Fig. 2). During the first phase of heating (up to 100°C) the mass loss for membrane A, and membrane E was 1.5% and 4.2% respectively. These mass losses can be attributed to the loss of loosely bound water molecules (14). The sequential increase of mass losses in this phase can be explained by the enhanced amount of hygroscopic materials (like sodium metasilicate, boric acid) in the compositions. Afterwards up to 300°C the mass losses for all the membranes were very less. During the second phase drastic falling in weight loss was observed after 300°C. As a consequence, membrane A and membrane E have shown 1.35% and 6.05% mass losses in between 300°C and 500°C. This phenomenon may be attributed to the fact that the boiling point of boric acid, whose composition was increased subsequently, is around

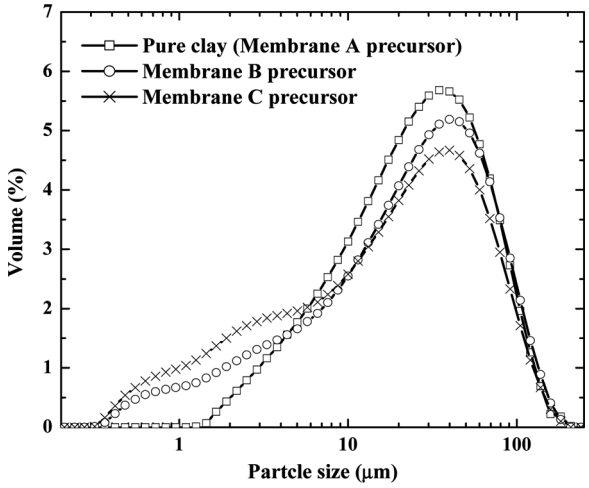


FIG. 1. Particle size distributions of different membrane materials (a) Membrane A, Membrane B and Membrane C materials (b) Membrane D, Membrane E and pure kaolin.

TABLE 2
XRF data of clay

| Main components in mass % | | | | | | | |
|---|---|---|---|---|---|---|---|
| Analyte | Na | Mg | Al | Si | K | Ca | Fe |
| Compound formulas | $Na_2O$ | MgO | $Al_2O_3$ | $SiO_2$ | $K_2O$ | CaO | FeO |
| Mass % | 2.065 | 1.518 | 17.097 | 71.595 | 1.901 | 1.465 | 3.236 |

| Trace components in mass % | | | | | | | | | |
|---|---|---|---|---|---|---|---|---|---|
| Analyte | P | S | Ti | Cr | Mn | Co | Ni | Cu | Cl |
| Compound formulas | $P_2O_5$ | $SO_3$ | $TiO_2$ | $Cr_2O_3$ | $MnO_2$ | $Co_3O_4$ | NiO | CuO | Cl |
| Mass % | 0.263 | 0.217 | 0.541 | 0.012 | 0.059 | 0.003 | 0.001 | 0.002 | 0.026 |

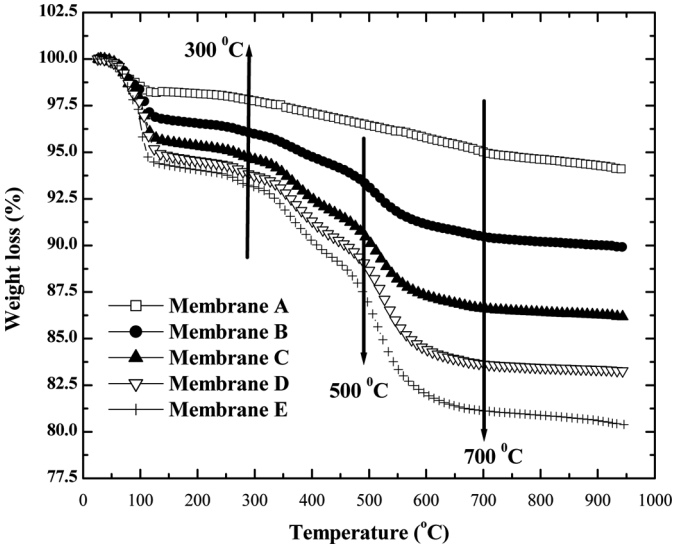


FIG. 2. Thermogravimetric analysis of the prepared membranes.

300°C. Afterwards, another strong fall in weight loss was observed after 500°C. In comparing with membrane B and membrane E, the mass loss in the range of 500°C to 700°C, was 2.83% and 7.28% consecutively. This was corresponding to the loss of structural hydroxyl groups at 513°C due to the transformation of kaolinite to metakaolinite according to the following reaction (19):

$$\underset{\text{(Kaolinite)}}{Al_2O_3 \cdot 2SiO_2 \cdot 2H_2O} \rightarrow \underset{\text{(metakaolinite)}}{Al_2O_3 \cdot 2SiO_2} + 2H_2O \qquad (6)$$

This phase change was not detected in membrane A since kaolin was not present in that composition. And finally, after 700°C, for all the compositions, mass changes were marginal. Thus, it can be concluded that the minimum sintering temperature for all the membranes should be above 700°C.

*X-Ray Diffraction Analysis*

For the 1000°C sintered membranes, reflections of quartz (Q), mullite (M), and nephiline ($Na_2O$, $Al_2O_3$, $2SiO_2$) (N) were detected (Fig. 3a). In case of membrane B, another characteristic reflection of corundum (C) was observed. Same types of peaks were observed by Löffler et al. (20) during dehydration of natural and synthetic goethite. Corundum is a crystalline form of aluminum

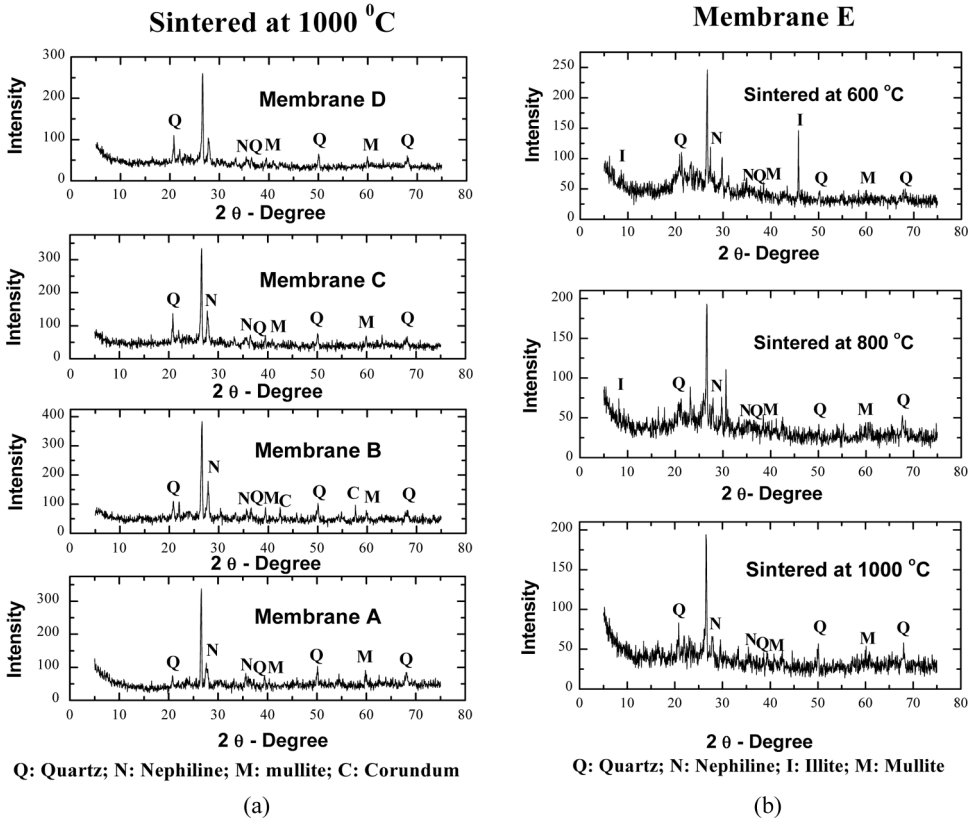


FIG. 3. XRD of prepared membranes (a) 1000°C sintered Membrane A, Membrane B, Membrane C and Membrane D. (b) Membrane E sintered at 600°C, 800°C and 1000°C.

oxide ($Al_2O_3$) with traces of iron, titanium, and chromium. In 1837, Gaudin made the first synthetic rubies (structure is very closer to corundum) by fusing alumina at a high temperature with a small amount of chromium as a pigment. As kaolin contains a large amount of aluminum oxide and the clay contains a very small amount of chromium (0.012%), titanium (0.541%), and iron (3.326%), so, the generation of corundum at higher sintering temperature was possible for membrane B, C, D, and E. However, for membrane C, D, and E, due to lower clay percentage in the composition (Table 1), may be the available chromium; titanium and iron were not enough for the generation of corundum. Temperature effects for phase changes were observed for membrane E (Fig. 3b). At 600°C sintered membrane, reflection of illite (I), nephiline (N), and quartz (Q) were observed. No reflection of kaolinite was found due to transformation to metakaolinite which was confirmed by the TGA experiment also. At the higher temperature sintered membranes (1000°C), no reflection of illite was observed. A comparable result was reported in the literature for Moroccan clay membranes (16). At higher temperature (800°C and 1000°C), mullite reflections were appearing, and quartz reflections did not change significantly. Thus, membrane A, C, D, and E contain mullite, quartz, and nephiline, whereas membrane B contains mullite, quartz, nephiline, and corundum.

*Surface Morphology and Pore Size Distribution from SEM Images*

To determine the area average pore size and the pore size distribution of the prepared membranes, morphological studies were conducted using SEM (Fig. 4). SEM also detects the small cracks on the membrane surface (if any). No such cracks were observed in any of the membranes. It was seen that with increasing the amount of kaolin in the membrane precursors, the structure was becoming denser. This was due to the fact that finer particles of kaolin were blocking the inter-particle space of clay, thus making the structure more condensed. Additionally, with the increase of the sintering temperature, the membrane became dense. SEM images from different sections of the membrane (and in different magnification) were considered and around 600 pore diameters from every membrane were measured using the ImageJ software (14). After opening the specific image in the software (File-->Open), first the scale of the original SEM image is related with the distance in pixel (Analyze-->Set scale). Afterwards, the pore diameters were measured by the tool ''Straight line selection''. The distance in pixels were converted to the known distance (micron) by the software itself. And finally, the measured data were transferred to MS-excel for further calculations. Average pore diameters ($d_s$) were calculated by the following Eq. (7)

$$d_s = \left[\frac{\sum_{i=1}^{n} n_i d_i^2}{\sum_{i=1}^{n} n_i}\right]^{0.5} \tag{7}$$

where $n$ is the number of pores, and $d_i$ is the pore diameter (μm) of the $i$th pore. With the decrease of the average particle size of the membrane preparing materials, the pore size was decreasing (Membrane A to Membrane E) (Fig. 5). The average pore size of membrane A and membrane D, sintered at 1000°C was 4.91 and 0.78 μm respectively (Table 3). This was due to the densification of the material. Similar results were reported by Das et al. (15) for membranes prepared from alumina. It was found that for a particular composition (membrane E), the pore size was increasing with the sintering temperatures. The reason was the overlapping of small pores creating large pores at higher sintering temperature. For membrane E, the average pore size was increased from 0.46 μm to 0.51 μm for corresponding sintering temperature of 850°C and 1000°C. A similar trend was reported by Saffaj et al. (16) for membranes prepared from Moroccan clay.

*Surface Pore Density*

Surface pore density corresponds to the average number of pores counted per unit area of the membrane surface. It was calculated from the SEM images and reported in Table 3. Pore density was increasing with the decrease of the particle size of membrane preparing materials. The pore density of membrane A and membrane D (sintered at 1000°C) were $2.47 \times 10^{10}$ and $1.24 \times 10^{11}\,m^{-2}$ respectively. As the size of the average particle sizes were decreasing, more number of particles were appearing within the same volume, hence the number of pores were increasing. Furthermore, for a particular composition, the pore density was decreased with increasing of the sintering temperatures. For membrane E, the pore density was decreased from $1.10 \times 10^{13}\,m^{-2}$ to $6.01 \times 10^{12}\,m^{-2}$ during the increasing of the sintering temperature from 850°C to 1000°C successively. This change was also representative of the overlapping of many small pores to a smaller number of large pores at higher sintering temperature.

*Water Permeability Experiment*

From the porosity values obtained by the pycnometric method, it was observed that porosity decreased with the decreasing of the average particle size of the membrane preparing materials. Membrane A and membrane D have shown a porosity of 0.38 and 0.29, respectively. This is due to the densification of the membrane structure. In the same way, it was increasing with the sintering temperature (Table 3). This was mainly due to squeezing of the membrane body during sintering and overlapping of small pores during the creation of large pores. Membrane E has

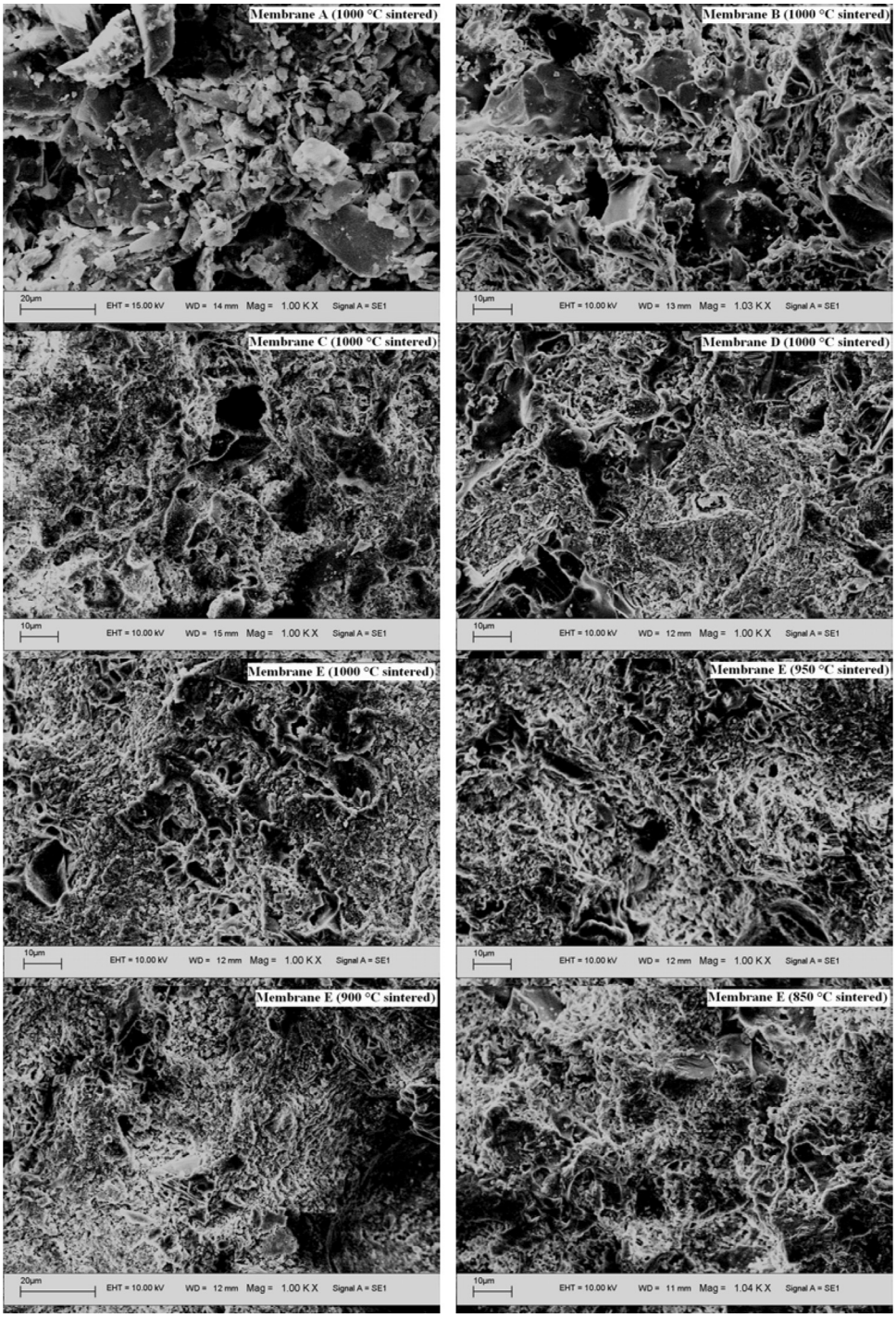


FIG. 4. SEM images of prepared membranes for different compositions and different sintering temperatures.

shown porosity of 0.22 and 0.26 for 850°C and 1000°C sintered samples successively.

The average pore diameter decreased with the smaller particle size (i.e with the increase of the kaolin percentage and decrease of the clay percentage) of membrane preparing materials and on the contrary, increased with the increase of the sintering temperature (Table 3). The average pore diameter obtained from membrane A and membrane D were 4.58 and 0.49 µm correspondingly. For membrane E, the values were 0.24 and 0.31 for 850°C and 1000°C sintered temperatures respectively. The pore size obtained from SEM images

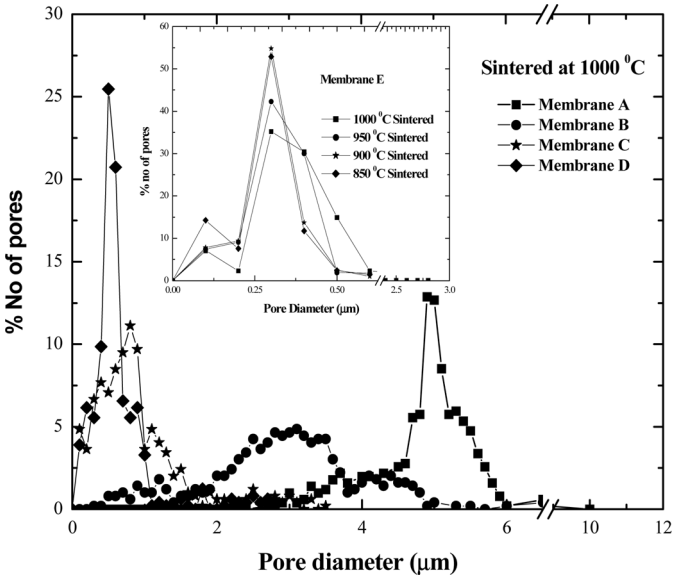


FIG. 5. Pore size distribution of prepared membranes.

was larger than from water permeability experiments. This was due to the presence of dead-end-pores which were incorporated in SEM image analysis but not integrated in the water permeability experiments. The average pore diameter, porosity, and water permeability are correlated by Eq. (2). Assuming the pores are cylindrical, the pore density is equal to the void volume per unit area divided by the volume of one pore.

From the determined pore sizes it can be forecasted that the higher pore size membranes (membrane A and B) can be applicable for surfactant-based separation like micellar enhanced microfiltration (MEMF) whereas comparatively lower pore size membranes (membrane C, D, and E) can be applicable for oily-wastewater separation or fruit juice clarification. Though the micelles having larger particle sizes which can be removed by filter paper, however, for large-scale separation, the filter paper option is unrealistic. The alternative ways for the separation of oil-water are: coagulation followed by flock forming, freeze-thaw, and electrochemical method, whereas fruit juice can be clarified by electro-flotation and enzyme based methodology. However, the advantages of using these prepared membranes over all those conventional processes are that these are low cost as well as less time consuming.

*Mechanical Strength*

The flexural strength was calculated by a three-point bending strength method and reported in Table 3. The flexural strength was increased with increasing sintering temperature. For membrane E, flexural strength increased from 7.01 MPa (850°C sintered) to 12.81 MPa (1000°C sintered). This is due to the formation of mullite and nephiline in the higher sintering temperatures. Similar results were reported by other researchers as well (14). Comparing with other compositions, membrane B has shown maximum mechanical strength (17.25 MPa). The reason behind this was the presence of corundum in the framework. As the XRD analysis of membrane A, C, and D was not showing much difference, it can be concluded that the higher strength of membrane C (15.45 MPa) and D (12.80 MPa), with respect to membrane A (11.55 MPa) were due to its more dense structure.

*Chemical Stability against Acid and Bases*

As an overall analysis, membranes have shown 2–10% weight loss during the treatments. The change in porosity, pore size, water permeability, and flexural strength were found to be marginal (Table 4). Thus all the membranes can be considered as chemically resistant. Membrane B has shown maximum chemical stability. The presence of corundum in the structure could be the reason for this.

TABLE 3
Different parameters of the prepared membranes

| Membrane | Sintering temperature (°C) | Average pore diameter: From SEM images (μm) | Average pore diameter: From water permeability (μm) | Porosity | Pore Density ($m^{-2}$) | Water permeability ($mPa^{-1}\,s^{-1}$) | Flexural strength (MPa) |
|---|---|---|---|---|---|---|---|
| Membrane A | 1000 | 4.91 | 4.58 | 0.38 | $2.47 \times 10^{10}$ | $4.98 \times 10^{-08}$ | 11.55 |
| Membrane B | 1000 | 3.11 | 2.28 | 0.37 | $1.24 \times 10^{11}$ | $1.20 \times 10^{-08}$ | 17.25 |
| Membrane C | 1000 | 1.10 | 0.71 | 0.35 | $1.37 \times 10^{12}$ | $1.10 \times 10^{-09}$ | 15.45 |
| Membrane D | 1000 | 0.78 | 0.49 | 0.29 | $2.45 \times 10^{12}$ | $4.35 \times 10^{-10}$ | 12.80 |
| Membrane E | 1000 | 0.51 | 0.31 | 0.22 | $4.80 \times 10^{12}$ | $1.32 \times 10^{-10}$ | 12.81 |
| | 950 | 0.48 | 0.29 | 0.24 | $6.01 \times 10^{12}$ | $1.26 \times 10^{-10}$ | 11.50 |
| | 900 | 0.48 | 0.27 | 0.25 | $7.76 \times 10^{12}$ | $1.14 \times 10^{-10}$ | 10.11 |
| | 850 | 0.46 | 0.24 | 0.26 | $1.10 \times 10^{13}$ | $9.36 \times 10^{-11}$ | 7.01 |

TABLE 4
Variation of different membrane parameters after chemical treatment

| Composition (Sintering temperatures,°C) | Weight loss (%) | Porosity | Pore Size (μm) | Permeability ($mPa^{-1}\,sec^{-1}$) | Flexural strength (MPa) |
|---|---|---|---|---|---|
| After acid treatment | | | | | |
| A (1000) | 5.37 | 0.42 | 4.68 | $5.63 \times 10^{-08}$ | 9.37 |
| B (1000) | 2.15 | 0.38 | 2.31 | $1.27 \times 10^{-08}$ | 14.44 |
| C (1000) | 4.38 | 0.37 | 0.73 | $1.23 \times 10^{-09}$ | 12.13 |
| D (1000) | 5.22 | 0.32 | 0.51 | $5.20 \times 10^{-10}$ | 12.86 |
| E (1000) | 6.05 | 0.26 | 0.32 | $1.66 \times 10^{-10}$ | 9.32 |
| E (950) | 6.63 | 0.29 | 0.29 | $1.52 \times 10^{-10}$ | 8.25 |
| E (900) | 8.23 | 0.32 | 0.28 | $1.57 \times 10^{-10}$ | 7.15 |
| E (850) | 9.38 | 0.34 | 0.25 | $1.33 \times 10^{-10}$ | 4.91 |
| After base treatment | | | | | |
| A (1000) | 6.89 | 0.43 | 4.71 | $5.72 \times 10^{-08}$ | 9.94 |
| B (1000) | 1.72 | 0.38 | 2.30 | $1.26 \times 10^{-08}$ | 14.32 |
| C (1000) | 2.83 | 0.37 | 0.72 | $1.23 \times 10^{-09}$ | 13.58 |
| D (1000) | 4.37 | 0.32 | 0.50 | $4.84 \times 10^{-10}$ | 13.15 |
| E (1000) | 5.65 | 0.26 | 0.31 | $1.56 \times 10^{-10}$ | 10.95 |
| E (950) | 7.13 | 0.30 | 0.30 | $1.69 \times 10^{-10}$ | 10.25 |
| E (900) | 8.41 | 0.32 | 0.28 | $1.57 \times 10^{-10}$ | 9.23 |
| E (850) | 10.02 | 0.35 | 0.25 | $1.37 \times 10^{-10}$ | 5.86 |



Chemical stability was increased with the higher sintering temperatures (Membrane E). This may be due to the formation of mullite and nephiline at the higher temperature sintered samples. The reason for the increasing porosity was due to the fact that- during the chemical treatment, some materials of the membrane were corroded thereby generating voids. Average pore size and permeability also increased. For membrane E (sintered at 1000°C), the pore diameter, porosity, permeability, and flexural strength were changed from 0.31 μm, 0.22, $1.32 \times 10^{-7}\,m^3m^{-2}\,kPa^{-1}\,sec^{-1}$ and 12.81 Mpa to 0.32 μm, 0.26, $1.66 \times 10^{-7}\,m^3m^{-2}\,kPa^{-1}\,sec^{-1}$ and 9.32 Mpa after acid treatment. The membrane has shown 6.05% weight loss.

## Variation of Average Pore Size and Pore Density

*Pore Size*

All the membranes were prepared from clay, kaoline, and binding materials without using any pore forming material like calcium carbonate. It was assumed that pores were created only by intra-particle spaces of the framework. Boric acid, sodium metasilicate, and sodium carbonate were used to generate hardness in the ceramic structure (8). Variation of the average pore diameter [$D_{avg}$] of the prepared membranes were compared with the average particle diameter [$D_{1,0}$], surface weighted mean [$D_{3,2}$], volume weighted mean [$D_{4,3}$], and specific area [$A_{sp}$] (Fig. 6). It is known that only the average mean particle diameter does not give a complete view of the statistical variation of the PSD. So, in general, it is advised to use some form of weighted mean diameter, where both particle quality (e.g., size, volume) and weighing (e.g., by number, area) relate the parameters of interest (17). The relationship of the average pore size with specific area was also considered due to the fact that the overall area of the particles was not represented by any of the above parameters.

It was observed that the pore diameter was decreasing with the decrease of the $D_{1,0}$, $D_{3,2}$, $D_{4,3}$ (Fig. 6). On the contrary, it was decreasing with the increase of the specific area. The average pore size was decreased from 4.6 μm to 0.3 μm for the value of the average particle diameter 34.66 μm to 17.51 μm. It was due to the fact that with the decrease of the particle size, more materials were aggregating within the volume, hence making the structure denser. Besides, specific area increases when the particle diameter decreases, and as a result the pore size also decreases. It was also seen that all the relationship can be represented by second-order polynomials (Eqs (8), (9), (10) and (11).) for which the $R^2$ values were found to be between 0.99 to 0.87.

$$D_{avg} = 9.35 - 0.89 \times D_{1,0} + 0.02 \times D_{1,0}^2 \tag{8}$$

$$D_{avg} = -3.8 + 1.1 \times D_{3,2} - 0.04 \times D_{3,2}^2 \tag{9}$$

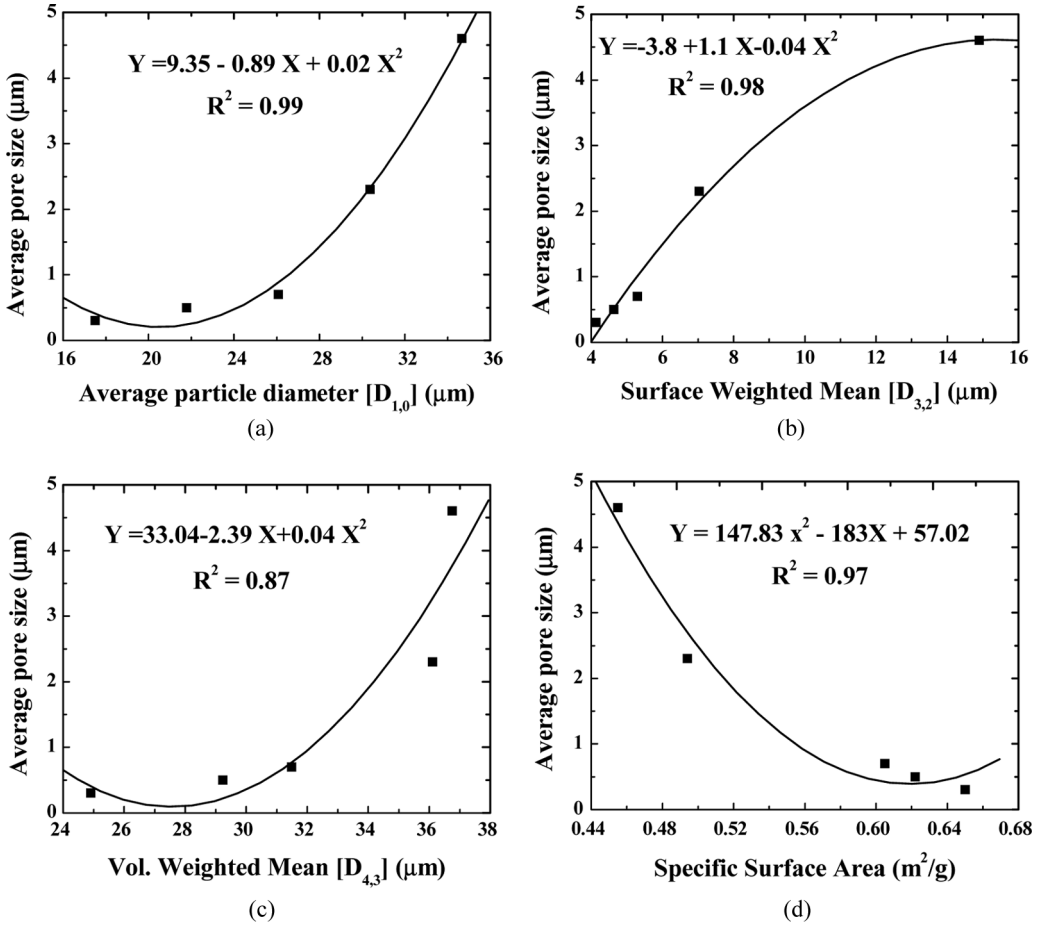


FIG. 6. Variation of average pore size with respect to (a) Average particle size, (b) Surface weighted mean, (c) Volume weighted mean and (d) Specific area.



$$D_{avg} = 33.04 - 2.39 \times D_{4,3} + 0.04 \times D_{4,3}^2 \quad (10)$$

$$D_{avg} = 57.02 - 183 \times A_{sp} + 147.83 \times A_{sp}^2 \quad (11)$$

The 95% confidence intervals for the developed relationships were shown in Table 5. As, the less difference between the upper and lower limit represent a better estimation, the coefficients of Eq. (9) have shown best among all the relationships. Depending on the confidence interval and $R^2$ values, the relationship with $D_{3,2}$ was found to be the best. These equations gave clear evidence that membrane pore sizes can be predicted from the membrane precursor PSD even before preparing the membrane.

*Pore Density*

For pore density [$N_p$], not only the average particle diameter, but the spread of the PSD also have strong influence over the pore diameter. To get an idea about this

TABLE 5
95% confidence intervals for the second order polynomials of average pore size with $D_{1,0}$, $D_{3,2}$, $D_{4,3}$, and $A_{sp}$

| | $D_{1,0}$ vs. $D_{avg}$ | | $D_{3,2}$ vs. $D_{avg}$ | | $D_{4,3}$ vs. $D_{avg}$ | | $A_{sp}$ vs. $D_{avg}$ | |
|---|---|---|---|---|---|---|---|---|
| | Lower | Upper | Lower | Upper | Lower | Upper | Lower | Upper |
| Constant term | −0.377 | 19.08 | −8.562 | 0.964 | −78.7 | 144.78 | −26.09 | 140.14 |
| Coefficient of linear term | −1.667 | −0.117 | −0.152 | 2.345 | −9.683 | 4.903 | −490.3 | 124.3 |
| Coefficient of quadratic term | 0.007 | 0.037 | −0.099 | 0.028 | −0.074 | 0.160 | −131.0 | 426.7 |

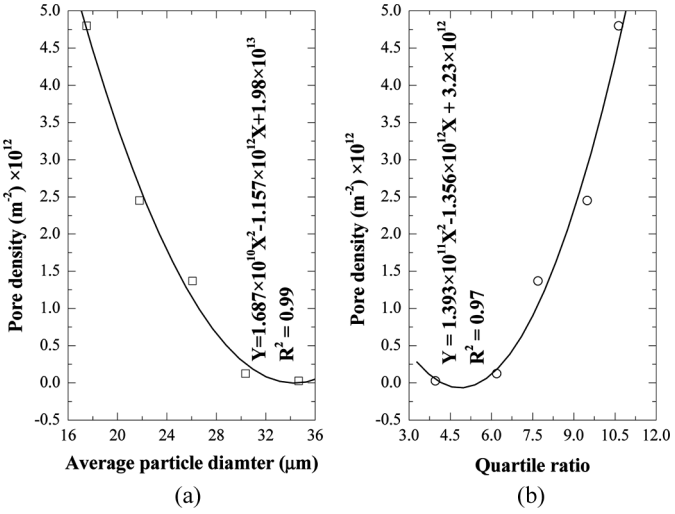


FIG. 7. Variation of pore density with respect to (a) Average particle size and (b) Quartile ratio.

spread of PSD, a simple way is to measure the difference between the particle sizes corresponding to the cumulative finer percentage of 75% and 25% in the PSD curve. Such a quantity is normally referred to as the quartile range and designated as "$_{25}X_{75}$" (21). The pore density was compared with the average particle diameter and quartile ratio (Fig. 7).

It was observed that the pore density was decreasing with the increase of the particle diameter. Pore density was decreased from $4.8 \times 10^{12}\,m^{-2}$ to $0.0247 \times 10^{12}\,m^{-2}$ for increase of the particle size from 17.51 μm to 34.66 μm. This aspect can be explained by the fact that during the agglomeration of the particles, more pores were forming. On the other hand, pore density was decreasing with the decrease of the quartile ratio. For the decrease of quartile ratio from 10.64 to 3.96, the pore density was decreased as mentioned above. Increase in the quartile ratio means, a wider PSD, more uneven distribution, hence

TABLE 6
95% confidence intervals for the second order polynomials of pore density with $D_{1,0}$, and $_{25}X_{75}$

| | $D_{1,0}$ vs. $N_p$ | | $_{25}X_{75}$ vs. $N_p$ | |
|---|---|---|---|---|
| | Lower | Upper | Lower | Upper |
| Constant term | $1.02 \times 10^{13}$ | $2.95 \times 10^{13}$ | $-5.62 \times 10^{12}$ | $1.21 \times 10^{13}$ |
| Coefficient of linear term | $-1.9 \times 10^{12}$ | $-3.9 \times 10^{11}$ | $-4.0 \times 10^{12}$ | $1.2 \times 10^{12}$ |
| Coefficient of quadratic term | $2.2 \times 10^{9}$ | $3.2 \times 10^{10}$ | $-3.7 \times 10^{10}$ | $3.2 \times 10^{11}$ |

TABLE 7
Cost analysis of the prepared membranes from the unit cost of raw materials

| Raw materials | | Clay | Kaolin | Sodium carbonate | Sodium metasilicate | Boric acid | Total cost ($/m$^2$) |
|---|---|---|---|---|---|---|---|
| | Unit price ($/kg) | – | 7.36 | 7.36 | 14.23 | 8.59 | |
| Membrane A | Material required* (m$^2$/kg) | 9.37 | 0.00 | 0.41 | 0.20 | 0.20 | – |
| | Cost/m$^2$ ($) | – | 0.00 | 3.00 | 2.90 | 1.75 | 7.65 |
| Membrane B | Material required* (m$^2$/kg) | 7.13 | 1.83 | 0.61 | 0.31 | 0.31 | – |
| | Cost/m$^2$ ($) | – | 13.50 | 4.50 | 4.35 | 2.62 | 24.97 |
| Membrane C | Material required* (m$^2$/kg) | 5.09 | 3.46 | 0.81 | 0.41 | 0.41 | – |
| | Cost/m$^2$ ($) | – | 25.50 | 6.00 | 5.80 | 3.50 | 40.79 |
| Membrane D | Material required* (m$^2$/kg) | 3.26 | 5.09 | 0.92 | 0.46 | 0.46 | – |
| | Cost/m$^2$ ($) | – | 37.49 | 6.75 | 6.52 | 3.94 | 54.70 |
| Membrane E | Material required* (m$^2$/kg) | 1.83 | 6.32 | 1.02 | 0.51 | 0.51 | – |
| | Cost/m2 ($) | – | 46.49 | 7.50 | 7.25 | 4.37 | 65.61 |

*5 cm diameter and 5 mm thick membrane were prepared from 20 g material.

an increase in the pore density. These relationships were also represented by second -order polynomials (Eq. (12) and (13)) with $R^2$ values of 0.99 to 0.97

$$N_p = 1.98 \times 10^{13} - 1.16 \times 10^{12} \times D_{1,0} + 1.69 \times 10^{10} \times D_{1,0}^2 \quad (12)$$

$$N_p = 3.23 \times 10^{12} - 1.36 \times 10^{12} \times ({}_{25}X_{75}) + 1.393 \times 10^{11} \times ({}_{25}X_{75})^2 \quad (13)$$

The calculated 95% confidence interval for all the developed second-order polynomials were shown in Table 6. Depending upon the $R^2$ values and confidence interval, the relationship of $N_p$ with $D_{1,0}$ was found better than the relationship with ${}_{25}X_{75}$. From these equations, it is clear that pore density can also be predicted from the PSD of the membrane preparing material.

### Cost Analysis

In general, ceramic membranes are ten times costlier than polymer membranes. Conventional industrial scale polymeric membranes are available for \$50–200/$m^2$ (22) and ceramic membranes for \$500–2000/$m^2$ (23). The thickness of the prepared membrane was 5 mm. The cost of the membrane per square meter is calculated on the basis of prices of the chemicals from corresponding companies (Table 7). The total material cost is varying from \$7.65/$m^2$ to \$65.61/$m^2$. Taking the cost of manufacturing and shipment, the cost may reach up to \$100–150/$m^2$, which is competitive with the cost of the polymer membranes.

## CONCLUSION

The aim of this work was to prepare microfiltration membranes from locally available clay and study the effect of inorganic precursors on the membrane morphology. Five numbers of microfiltration membranes were prepared with different compositions of clay, kaolin, and other binding materials. It was found that with the increase of sintering temperature, the pore size as well as permeability and flexural strength were increasing while the porosity and pore density were decreasing. It was observed that the initial average particle size of the membrane precursor is the key factor for controlling the pore size and pore density of the membrane. The pore size of the membrane was related to the average particle diameter [$D_{1,0}$], surface weighted mean diameter [$D_{3,2}$], volume weighted mean diameter [$D_{4,3}$], and the specific area whereas the pore density was related with the average particle diameter [$D_{1,0}$] and quartile ratio [${}_{25}X_{75}$]. It can be concluded that the pore diameter and density can be predicted directly from the particle size distribution of membrane precursors. The prepared membranes can be useful for MEMF, oil-water separation, or fruit juice clarification depending upon the pore sizes. Membrane based separation is better than the standard methods available, due to low cost, less time consuming, and high efficiency.

## REFERENCES


1. Parnham, C.S.; Davis, R.H. (1996) Protein recovery from bacterial cell debris using crossflow microfiltration with backpulsing. *J. Membr. Sci.*, 118: 259–268.
2. Song, C.; Wang, T.; Pan, Y.; Qiu, J. (2006) Preparation of coal-based microfiltration carbon membrane and application in oily wastewater treatment. *Sep. Purif. Technol.*, 51: 80–84.
3. Nandi, B.K.; Das, B.; Uppaluri, R.; Purkait, M.K. (2009) Microfiltration of mosambi juice using low cost ceramic membrane. *J. Food Engg.*, 95: 597–605.
4. Urkiaga, A.; Fuentes, L.; De, L.; Acilu, M.; Uriarte, J. (2002) Membrane comparison for wine clarification by microfiltration. *Desalination*, 148: 115–120.
5. Sikder, J.; Pereira, C.; Palchoudhury, S.; Vohra, K.; Basumatary, D.; Pal, P. (2009) Synthesis and characterization of cellulose acetate-polysulfone blend microfiltration membrane for separation of microbial cells from lactic acid fermentation broth. *Desalination*, 249: 802–808.
6. Almandoza, M.C.; Marchese, J.; Prádanos, P.; Palacio, L., Hernández, A. (2004) Preparation and characterization of non-supported micro-filtration membranes from aluminosilicates. *J. Membr. Sci.*, 241: 95–103.
7. Wang, Y.H.; Xing, Liu X.Q.; Meng, G.Y. (2007) Preparation of asymmetric pure titania ceramic membranes with dual functions. *Matl Sci. Engg.*, 445–446: 611–619.
8. Reed, J.S. (1995) *Principles of Ceramics Processing,* 2nd Ed.; John Wiley & Sons: NewYork.
9. DeFriend, K.A.; Wiesner, M.R.; Barron, A.R. (2003) Alumina and aluminate ultra-filtration membranes derived from alumina nanoparticles. *J. Membr. Sci.*, 224: 11–28.
10. Falamaki, C.; Shafiee, A.M.; Aghaie, A. (2004) Initial sintering stage pore growth mechanism applied to the manufacture of ceramic membrane supports. *J. Eur. Ceram. Soc.*, 24: 2285–2292.
11. Wang, Y.H.; Tian, T.F.; Liu, X.Q.; Meng, G.Y. (2006) Titania membrane preparation with chemical stability for very hash environments applications. *J. Membr. Sci.*, 280: 261–269.
12. Masmoudi, S. ; Larbot, A. ; Feki, H.E. ; Amara, R.B. (2007) Elaboration and characterisation of apatite based mineral supports for microfiltration and ultrafiltration membranes. *Ceram. Int.*, 33: 337–344.
13. Khemakhem, S.; Larbot, A.; Ben Amar, R. (2009) New ceramic microfiltration membranes from Tunisian natural materials: Application for the cuttlefish effluents treatment. *Ceram. Int.*, 35: 55–61.
14. Nandi, B.K.; Uppaluri, R.; Purkait, M.K. (2008) Preparation and characterization of low cost ceramic membranes for micro-filtration applications. *Appl. Clay Sci.*, 42: 102–110.
15. Das, N.; Maiti, H.S. (1999) Effect of size distribution of the starting powder on the pore size and its distribution of tape cast alumina microporous membranes. *J. Europ. Cer. Soc.*, 19: 341–345.
16. Saffaj, N.; Persin, M.; Younsi, S.A.; Albizane, A.; Cretin, M.; Larbot, A. (2006) Elaboration and characterization of microfiltration and ultrafiltration membranes deposited on raw support prepared from natural Moroccan clay: Application to filtration of solution containing dyes and salts. *Appl. Clay Sci.*, 31: 110–119.
17. Merkus, G.M. (2009) *Particle Size Measurements: Fundamentals, Practice, Quality*; Springer.
18. Chesworth, W. (2008) *Encyclopedia of Soil Science*; Springer.

19. Chena, Y.F.; Wang, M.C.; Hon, M.H. (2006) Phase transformation and growth of mullite in kaolin ceramics. *J. Afr. Earth Sci.*, 46: 245–252.
20. Löffler, L.; Mader, W. (2005) Anisotropic X-ray diffraction peak broadening and twinning in diaspore-derived corundum. *J. Europ. Ceram. Soc.*, 25: 639–648.
21. Allen, T. (1981) *Particle Size Measurement*; Chapman & Hall: London, New York.
22. Bhide, B.D.; Stern, S.A. (1991) A new evaluation of membrane processes enrichment of air. II. Effects of economic membrane properties. *J. Membr. Sci.*, 62: 37–58.
23. Koros, W.J.; Mahajan, R. (2000). Pushing the limits on possibilities for large scale gas separation: which strategies? *J. Membr. Sci.*, 175: 181–196.